# Optical selection rule for the lower Davydov excitons in co-oligomer single crystals

Kazuki Bando,* Toshiteru Nakamura, Seiji Fujiwara, and Yasuaki Masumoto
*Institute of Physics and Center for Tsukuba Advanced Research Alliance (TARA), University of Tsukuba, Tsukuba 305-8571, Japan*

Fumio Sasaki and Shunsuke Kobayashi
*Photonics Research Institute, National Institute of Advanced Industrial Science and Technology (AIST), Tsukuba 305-8568, Japan*

Yukihiro Shimoi
*Nanotechnology Research Institute, National Institute of Advanced Industrial Science and Technology (AIST), Tsukuba 305-8568, Japan*

Shu Hotta
*Department of Macromolecular Science and Engineering, Graduate School of Science and Technology, Kyoto Institute of Technology, Kyoto 606-8585, Japan*

(Received 4 October 2007; published 15 January 2008)

Intrinsic optical transitions of lower Davydov excitons in thiophene/phenylene co-oligomer (TPCO) crystals were investigated. Lower Davydov excitons are either optically allowed or forbidden depending on the number of thiophene rings constituting the TPCOs. The TPCO molecules are orientated nearly parallel to each other like *H* aggregates and are aligned in herringbone fashion within a crystalline layer. The transition selection rules are dominated by the components of the molecular transition dipole moments lying in the herringbone planes of the respective crystals. The selection rules at the exciton band bottoms of the TPCOs differ from those of oligothiophenes in spite of these two compounds having similar molecular structures. The selection rules vary drastically with the molecular alignment because of the *H* aggregation. TPCO and oligothiophene crystals are treated as *H* aggregates as a first approximation. This treatment is very useful for understanding the optical transitions of conjugated materials.

DOI: 10.1103/PhysRevB.77.045205 PACS number(s): 71.35.Cc, 78.40.Me, 78.55.Kz

## I. INTRODUCTION

Conjugated organic semiconductors have received considerable attention as materials for optical and electronic devices in recent years. A critical issue for the development of such devices is the control of molecular alignment in materials. Since the molecular alignment in conjugated organic semiconductors is expected to strongly influence their optical and electrical properties, oligomers are considered to have more potential than polymers in these organic materials. This is because the shorter conjugation length of oligomers places fewer restrictions on the molecular alignment upon crystallization. Oligomer crystals are thus expected to exhibit optical phenomena due to the anisotropic and coherent natures of their crystals.

A lot of oligomers crystallize in herringbone (HB) fashion, so that they can be considered to be two-dimensional *H* aggregates in a broad sense. In *H* aggregates (in the narrow definition of that phrase) the molecular transition dipole moments ($\mu$'s) are antiparallel to each other so that their sum cancels out at the lowest excited states. Thus, their optical transitions are forbidden. In spite of oligomer crystals having molecular alignments similar to that of *H* aggregates, their optical transitions are not forbidden. In addition, pronounced optical phenomena including amplified spontaneous emission[1,2] and excitonic superradiance[3] have been observed in several oligomer crystals. Oligothiophene (OT) crystals, which are typical oligomers, have been investigated for a considerable time in order to gain a deeper understanding of the optical properties of oligomers.[4–8] Meanwhile, the good emissive properties of oligomers have been well interpreted using the pinwheel aggregate model recently developed by Spano;[9–12] this model is applicable to many oligomers. In oligomers possessing an off-axis component of the molecular transition dipole moment ($\mu_\perp$), $\mu_\perp$ is orientated in HB fashion within a crystalline layer. In the pinwheel aggregate model, the optical transitions in oligomer crystals are considered to be driven by constructive or destructive interference between the $\mu_\perp$'s of two translationally nonequivalent molecules aligned in HB fashion. In fact, the pinwheel aggregate model successfully predicted that the lowest excited states of OT crystals are optically allowed in the case of even numbers of thiophene rings.[13] On the other hand, they are optically forbidden in the case of odd-numbered OTs possessing no $\mu_\perp$. Thus, optical transitions in oligomer crystals sensitively depend on the directions of the $\mu$'s of the molecules aligned like *H* aggregates. Furthermore, the aggregate model has successfully predicted the other detailed optical properties of OT crystals.[14–16]

Recently many hybridized oligomers consisting of different conjugated monomers have been synthesized. Since there are a large number of different combinations of monomers, it is possible to develop molecules possessing desired structures, conjugation lengths, and $\mu$'s by selectively choosing the combination. In particular, thiophene/phenylene co-oligomers (TPCOs), which consist of thiophenes and phenylenes, have received considerable attention.[17–20] One TPCO, 2,5-bis(4-biphenylyl)-thiophenes (BP*n*T: $n=1-4$) consists of one, two, three, or four thiophene rings with two phenylene rings at both ends of the molecule[17,18] and its molecules are aligned in HB fashion in crystals. These BP*n*T crystals exhibit good electrical properties,[21] and inter-

 ©2008 The American Physical Society

esting optical phenomena such as high-gain amplified spontaneous emission,[22–24] lasing by a self-formed cavity,[25,26] and pulselike emission with a time delay suggesting superfluorescence.[27] These optical phenomena are observed in BP*n*Ts whose structures differ slightly from those of OTs. Thus, drastic changes to the optical properties can be effected by making slight changes to their structures. In this paper, we report the fundamental optical transitions of BP*n*T crystals of $\pi$-conjugated materials and the interpretation of them.

## II. EXPERIMENTAL DETAILS

Freestanding BP*n*T ($n=1-4$) crystals were prepared, and photoluminescence (PL) and absorption measurements were performed. The crystals were grown in the vapor phase in an environmental gas at atmospheric pressure at growth temperatures in the range 300–400 °C.[22] The BP*n*T ($n=1-4$) crystalline powders were encapsulated in nitrogen gas using glass ampoules. The glass ampoules were heated in a furnace at 300–400 °C, with the top ends of the ampoules being out of the furnace. The temperature gradient between the top and the bottom of the ampoules drove convective flow of the environmental gas in the ampoules. This convective gas flow caused freestanding crystals to grow within the appropriate temperature region inside the ampoules. Single thin BP*n*T ($n=1-4$) crystals formed in the ampoules and they were a few millimeters in lateral size and they had thicknesses ranging from several microns to several tens of microns. Transmission electron microscopy was used to obtain electron diffraction patterns from single crystals.

Optical absorption and PL measurements were performed at 10 K. A He-Cd continuous-wave laser (wavelength: 325 nm) was used as a light source for the PL measurements, while a halogen lamp and a Xe lamp were used for the absorption measurements. The incident light beams were normal to the *a*-*b* planes, which were in close contact with quartz substrates. The PL was detected using a monochromator and a liquid-nitrogen-cooled charge-coupled device. The excited states of isolated BP*n*T molecules were calculated using the semiempirical quantum chemical method ZINDO/S implemented in GAUSSIAN03.[28] The geometrics of the molecules are fixed to those of their crystal structures.[19,20,29] We confirmed that the first singlet excited states are optically allowed in these molecules.

## III. RESULTS AND DISCUSSION

### A. Photoluminescence and absorption spectra

Figure 1(a) shows nonpolarized PL and absorption spectra of the BP*n*T ($n=1-4$) crystals at 10 K. For the purpose of comparison, the energy scales of spectra are shifted in order to align the vibronic sidebands vertically. The vibronic sidebands indicated by dashed lines are shifted from the center by ~180 meV by the $A_1$ and $A_g$ modes of the odd- and even-numbered BP*n*T crystals, respectively.[24,30] These optical spectra of the BP*n*T crystals are very similar to each other because of the vibronic progressions, as is seen in Fig. 1(a). However, pronounced sharp peaks are visible around

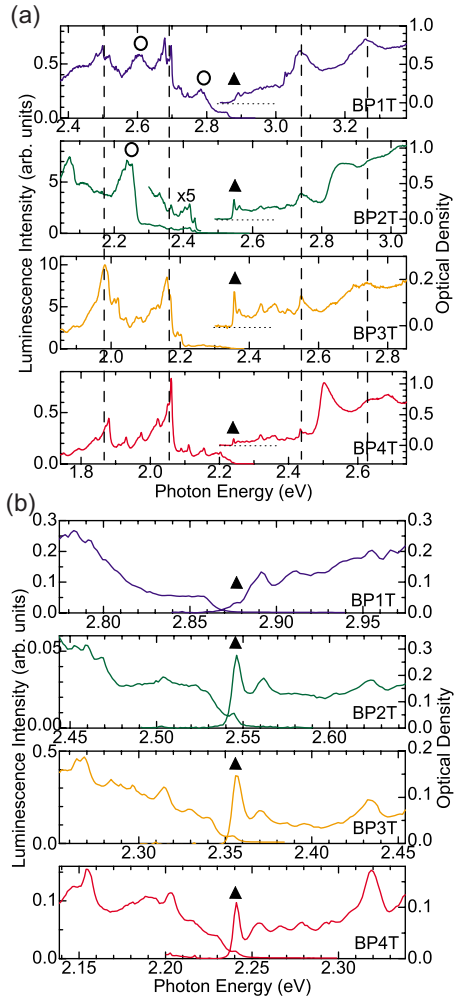


FIG. 1. (Color online) (a) Nonpolarized PL and absorption spectra of BP*n*T ($n=1-4$) crystals. Triangles indicate the 0-0 lower Davydov exciton transition energies and dashed lines show their progressive vibronic sidebands. The energy scales of spectra are shifted in order to align the 0-0 exciton transition energies. The PL intensity scales are normalized to 10 at the maximum peak of the BP3T for the purpose of comparison. (b) Enlarged PL and absorption spectra of the BP*n*T ($n=1-4$) around the 0-0 exciton transitions.

the absorption edge for BP*n*T ($n=2-4$), while a relatively small shoulder is seen in the spectrum of BP1T, as indicated by triangles in Fig. 1(a). Expanded spectra in the vicinity of the center are shown in Fig. 1(b). Small shoulders are observable in the PL spectrum of BP*n*T ($n=2-4$), whereas there is no observable structure in that of BP1T for the energy range shown in Fig. 1(b). The center peaks are assigned to the nonvibronic (0-0) transitions of the lower Davydov excitons on the basis of the mirror symmetry of the PL and absorption spectra.[24] However, the center peaks exhibit small Stokes shifts of 1.5 meV (BP2T), 1.9 meV (BP3T), and 0.3 meV (BP4T), which arise from so-called *X* traps[31] caused by crystal imperfections. That suggests efficient energy transfer in exciton bands.[32] In passing, PL bands labeled by open circles are due to extrinsic origins in the crystal, such as aggregates of the molecules or defects in the

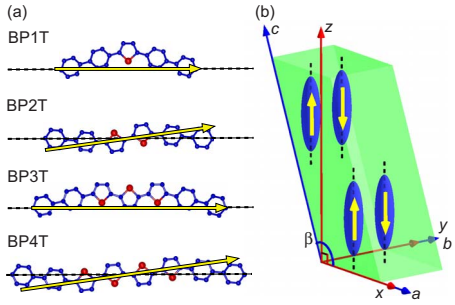


FIG. 2. (Color online) (a) Molecular structures and transition dipole moments of BP$n$Ts ($n$=1–4). Dashed lines denote the long molecular axes and arrows indicate the transition dipole moments. (b) Relationship between a monoclinic system and the orthogonal coordinate system defined in the text. The parallelepiped show the unit cell structure of the monoclinic system and the spheroids indicate the BP$n$T molecules. The long molecular axes and the transition dipole moments are drawn to be perpendicular to the $a$-$b$ plane for simplicity.

crystals.[24] Although extrinsic PL bands predominate in the PL spectrum of BP2T crystals, there is a weak intrinsic 0-0 transition in this spectrum.

### B. Estimation of molecular transition dipole moments

Excitonic optical transitions in oligomer crystals are controlled by the alignments of the $\mu$'s between the ground state and the first excited state of the isolated molecules. The $\mu$'s, in turn, are dependent on the molecular symmetry. BP$n$T oligomers are planar molecules, and those having odd $n$ and even $n$ belong to point groups $C_{2v}$ and $C_{2h}$, respectively.[19,20] Figure 2(a) shows the molecular structures of BP$n$T ($n$=1–4), and the arrows indicate the $\mu$'s derived from the point groups. Figure 2(a) shows that the $\mu$'s of the odd-numbered BP$n$Ts are aligned with the long molecular axes, which are defined as the lines that connect the two terminal carbons (dashed lines). On the other hand, the $\mu$'s of the even-numbered BP$n$Ts lie in the molecular planes, but deviate slightly from the long molecular axes. The OTs have the same features as the BP$n$Ts with respect to the direction of the $\mu$'s, because the point groups of the odd- and even-numbered OTs are the same as those of the BP$n$Ts.[13–16]

However, actual BP$n$T molecules in crystals are distorted, reducing their molecular symmetries.[19,20] Odd-numbered BP$n$T molecules are slightly bow shaped with the biphenylyl planes on either side slightly bent and twisted with respect to the thiophene plane. However, the BP1T molecule still practically belongs to the point group $C_s$ resulting in the $\mu$ lying along the long molecular axis, despite its reduced symmetry. Thus, the $\mu$ of BP1T should be perfectly aligned with the long molecular axis. By contrast, although the symmetry of the BP3T molecule is lower than $C_s$, its deviation from $C_s$ is negligibly small. Thus, $\mu$ of BP3T can also be considered to be aligned with the long molecular axis. In the case of the even-numbered BP$n$T molecules, although their symmetries are also lower than $C_{2h}$, the deviation from $C_{2h}$ is also relatively small.

The BP$n$T crystal structures belong to monoclinic $P2_1/n$ and $P2_1/c$ space groups for $n$=1,4 and $n$=2,3, respectively.[19,20] The unit cell structure of the BP$n$T crystals is schematically shown in Fig. 2(b), where the distinction between the two space groups can be ignored since it does not affect the present discussion. The parallelepiped and the spheroids in this figure represent the unit cell structure of the monoclinic system and the BP$n$T molecules, respectively. In addition, the axes of the orthogonal coordinate system used to calculate the $\mu$'s are depicted by arrows in Fig. 2(b) (see description later). The long molecular axes are drawn vertical to the $a$-$b$ plane in Fig. 2(b) for simplicity. The BP$n$T molecules in the crystals are aligned like the $H$ aggregate and the projections of the molecules onto the $a$-$b$ planes are aligned in HB fashion. Since the BP$n$T crystals have four molecules in their unit cells as shown in Fig. 2(b), the molecular electronic levels in the crystals are split into four Davydov excitonic bands. The four bands split by the $C_1$ site symmetries of the BP$n$T crystals consist of $a_g$ and $a_u$ components on the low-energy side and $b_g$ and $b_u$ components on the high-energy side, in the same manner as sexithiophene.[4] The optically allowed $a_u$ and $b_u$ components arise from the interaction between the two nonequivalent molecules in the unit cell in the same layer. The $a_u$ and $b_u$ components correspond to the lower and upper Davydov exciton bands, respectively. In the present paper, we consider only the $a_u$ excitonic bands of the lowest optically allowed transitions in the crystals. The optical transitions are dominated by the $\mu$'s of the two nonequivalent molecules in the HB plane, as discussed below.

We estimated the normalized $\mu$ vector of one of the two nonequivalent molecules in each crystal using the ZINDO/S semiempirical method; the other one can be estimated by applying symmetry operations of the monoclinic space groups. Table I gives the normalized $M$ vectors of the long molecular axes, the normalized $\mu$ vectors, the magnitude of the $\mu$'s, and the angle $\theta$ between two vectors. They were evaluated on the basis of the atomic positional parameters obtained by x-ray diffraction,[19,20] where the atomic positions were transformed to the orthogonal $xyz$ coordinate system shown in Fig. 2(b). The $x$, $y$, and $z$ axes are defined as the $a$ axis, $b$ axis, and the axis perpendicular to $a$-$b$ plane of each crystal, respectively, as shown in Fig. 2(b). Since the estimations of the $M$'s and the $\mu$'s are performed by using the experimentally measured atomic positions, the distortion of the molecules in the crystals is taken into consideration in these estimations. However, the estimated $\mu$ vector of BP1T is not correct. Although the $\mu$ of BP1T should be perfectly aligned with the long molecular axis because of the molecular symmetry $C_s$, as discussed above, the estimated angle $\theta$ between them is not zero, Table I shows. This discrepancy is relatively large for the shorter molecules such as BP1T, because the BP$n$Ts are linear $\pi$-conjugated molecules possessing $\mu$'s aligned with the long molecular axes. In fact, as Table I shows, the $\theta$ of BP1T is larger than that of BP3T, even if BP3T also has a discrepancy. In the case of the odd-numbered BP$n$Ts, the normalized $M$ vectors are regarded as the true normalized $\mu$ vectors on the basis of the symmetry of the molecules in the following discussion. On the other hand, reconsideration is not needed in the case of the $\mu$'s of

TABLE I. Normalized vectors of the long molecular axes of the molecules ($M$), normalized vectors of the transition dipole moments ($\mu$), magnitudes of the $\mu$'s, and the angle $\theta$ between the $\mu$ and the $M$ in BP$n$T ($n=1-4$) crystal structures.

| | $M_x/M$ | $M_y/M$ | $M_z/M$ | $\mu_x/\mu$ | $\mu_y/\mu$ | $\mu_z/\mu$ | $\mu$ (D) | $\theta$ (deg) |
|---|---|---|---|---|---|---|---|---|
| BP1T | −0.018 | 0.002 | 1.000 | −0.030 | −0.024 | 0.999 | 12.0 | 1.7 |
| BP2T | −0.022 | −0.001 | 1.000 | 0.092 | 0.024 | 0.996 | 12.5 | 6.7 |
| BP3T | −0.042 | −0.016 | 0.999 | −0.052 | −0.023 | 0.998 | 13.8 | 0.7 |
| BP4T | −0.032 | 0.001 | 1.000 | 0.058 | −0.010 | 0.998 | 14.8 | 5.2 |

the even-numbered BP$n$Ts, since the intrinsic deviations of the $\mu$'s from the long molecular axes are larger than the discrepancy.

### C. Interpretation of optical transitions in the crystals

The selection rules for the optical transitions of the 0-0 lower Davydov excitons in the BP$n$T crystals shown in Fig. 1(b) can be explained by the model developed by Spano for the optical transitions of oligomer crystals with molecules aligned in HB fashion.[9–12] This model successfully predicted the optical transitions in OT crystals.[13–16,33] In this model, the optical transitions are driven by constructive or destructive interference of $\mu$'s aligned in HB fashion. In such oligomer crystals, the molecules are aligned nearly parallel to each other like $H$ aggregates in a HB plane. Therefore, at lower Davydov levels, the $\mu$'s of nonequivalent molecules in a HB plane are almost antiparallel to each other and cancel out. In the same way, the $\mu$'s of BP$n$T molecules in a HB plane are also almost antiparallel to each other at the lower Davydov levels. However, the actual $\mu$'s of nonequivalent molecules are not completely antiparallel to each other. Figure 3 shows schematic drawings of the alignment of BP$n$T molecules in a HB plane. The spheroids represent the BP$n$T molecules, the dashed lines indicate the long molecular axes, and the arrows denote the $\mu$'s. Figure 3(a) shows a perspective view of the molecular alignment in a HB plane. The two nonequivalent molecules are inclined slightly in different directions to each other and their $\mu$'s are also not perfectly antiparallel to each other, as Fig. 3(a) shows. The $x$-$y$, $x$-$z$, and $y$-$z$ plane views of the alignment are shown schematically in Figs. 3(b)–3(d), respectively. In this figure, the two molecules inside the square are the nonequivalent molecules. They are orientated in different directions from each other in the $x$-$y$ plane. On the other hand, both the monoclinic $P2_1/n$ and $P2_1/c$ space groups of the BP$n$T crystals result in parallel alignments of the molecules on the projection onto the $x$-$z$ plane [see Fig. 3(c)]. Therefore, the projections of the nonequivalent $\mu$'s onto the $x$-$z$ plane are perfectly antiparallel to each other, even though the $\mu$'s are not completely antiparallel to each other. By contrast, the projections of the $\mu$'s onto the $y$-$z$ plane are not antiparallel to each other as Fig. 3(d) shows. Therefore, both the $\mu_x$'s and the $\mu_z$'s destructively cancel out but only the $\mu_y$'s constructively interfere at the lower Davydov levels. As a result, the optical transitions of the lower Davydov excitons in any BP$n$T crystal should be driven by the $\mu_y$'s.

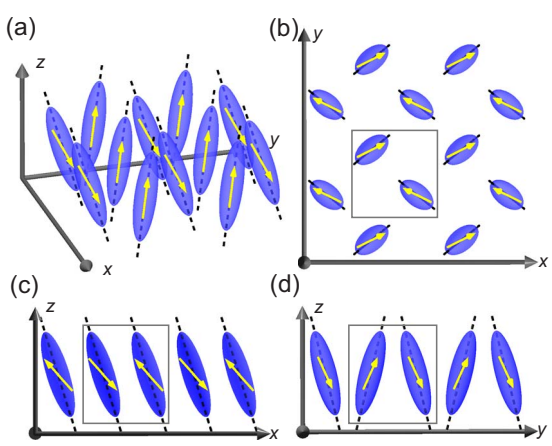


FIG. 3. (Color online) Schematic drawings of the alignment of the BP$n$T molecules in a HB plane. The alignments are expressed in the orthogonal coordinate system. The spheroids represent the BP$n$T molecules, the dashed lines indicate the long molecular axes, and the arrows represent the transition dipole moments. (a) Perspective view of the alignment of the BP$n$T molecules; (b) $x$-$y$ plane view; (c) $x$-$z$ plane view; (d) $y$-$z$ plane view.

The $x$-$y$ plane views of the alignments of the BP$n$T ($n=1-4$) molecules in respective HB planes are shown schematically in Figs. 4(a)–4(d), where the $\mu$'s are indicated by arrows. In addition, the directions of the $\mu_z$'s are also denoted by plus and minus signs in Figs. 4(a)–4(d). The $\mu$'s drawn in Fig. 4 are the $\mu$ vectors for even $n$ and the $M$ vectors for odd $n$ (see Table I). The nonequivalent molecules in all BP$n$T crystals are orientated in different directions from each other in the $x$-$y$ plane (see Fig. 4). However, as mentioned above, when discussing the optical transitions at the lower Davydov levels it is only necessary to consider the $\mu_y$'s. In fact, the $\mu_y$'s of the BP$n$Ts are 0.024 D (BP1T), 0.300 D (BP2T), 0.221 D (BP3T), and 0.148 D (BP4T). The $(\mu_y/\mu)^2$ of the BP1T crystal is 2 orders of magnitude smaller than that of the BP$n$T ($n=2-4$) crystals (see Table I). Therefore, the lower Davydov exciton in the BP1T crystal should exhibit a much weaker optical transition than those in the BP$n$T ($n=2-4$) crystals. This prediction is actually in good agreement with the experimental results shown in Fig. 1(b). On the other hand, vibronic sidebands should be observed independently of the transition selection rules for the 0-0 lower Davydov excitons, unless the Huang-Rhys factor is zero.[9,11,13] In fact, vibronic sidebands appear in all the BP$n$Ts as indicated by the dotted lines in Fig. 1(a).

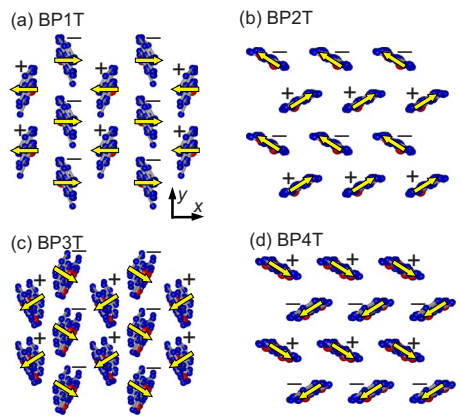


FIG. 4. (Color online) HB planes and transition dipole moments of BP$n$Ts ($n$=1–4). The arrows show the directions of the transition dipole moments in the HB planes. The plus and minus signs indicate the off-plane component of the transition dipole moments.

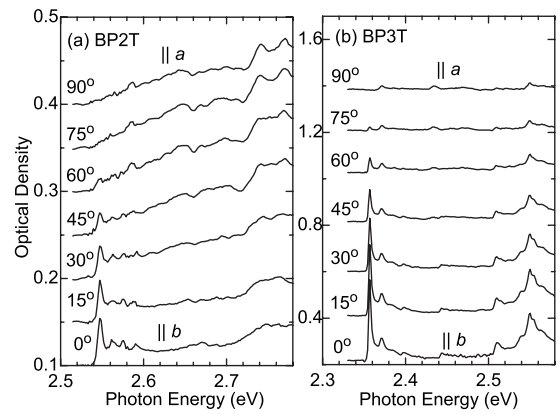


FIG. 5. Linearly polarized absorption spectra of (a) BP2T and (b) BP3T crystals. The polarization direction was rotated in the $a$-$b$ plane from the $b$ axis to the $a$ axis by the oblique angle denoted in these figures.

It should be noted that the transition selection rules for the 0-0 lower Davydov excitons in the BP$n$T crystals differ from those for OT crystals in spite of the similarity of these molecules. The lower Davydov excitons in any odd-numbered OT are optically forbidden.[13,14] However, the lower Davydov exciton in the BP3T crystal is optically allowed regardless of the oligomer having an odd number of thiophene rings. On the other hand, the transition selection rules for the BP$n$Ts ($n$=1,2,4) correspond to those for OTs depending on the number of thiophene rings. This difference is explained below. The long molecular axes of the two nonequivalent molecules in the BP$n$T crystals are inclined slightly with each other in the opposite direction to the $y$ axis as shown in Fig. 3(d). The inclinations of the BP$n$Ts ($n$=1,2,4) are negligibly small. However, that of BP3T is relatively large. In fact, the $M_y/M$ of BP3T is 1 order of magnitude larger than those of the other BP$n$Ts (see Table I). Therefore, only the $\mu_y$'s in the BP3T crystal do not vanish even if the BP3T possesses the same molecular symmetry as the odd-numbered OTs and BP1T. That is why the lower Davydov exciton in the BP3T crystal is optically allowed in spite of it being an odd-numbered BP$n$T. By contrast, the lower Davydov exciton in the BP1T crystal is optically forbidden because of the negligible inclination of the $\mu$'s in the same manner as those in the odd-numbered OTs. In addition, the lower Davydov excitons in the even-numbered BP$n$T crystals are also optically allowed in the same manner as those in the even-numbered OTs.

Thus, since the $\mu$'s in the BP$n$T crystals are nearly aligned like $H$ aggregates, the inclinations of the $\mu$'s from the $z$ axis to the $y$ axis are much smaller, as Table I shows. However, the optical transitions are very sensitive to the inclinations even though the inclinations are very small. This implies that optical transitions of such oligomer crystals can be controlled by varying the inclinations of their $\mu$'s. In other words, oligomer crystals possessing tailored optical performances can be developed by controlling the molecular alignments in the crystals; the molecular alignments can be controlled by doing things such as adding side chains to the oligomers.

### D. Polarization dependence

Based on the aggregate model, the optical transitions of the lower Davydov excitons in BP$n$T crystals should be driven by their $\mu_y$'s, as described above. Therefore, the optical transitions of the lower Davydov excitons should be polarized along the $y$ axis, where the $y$ axis corresponds to the $b$ axis of the crystals [see Fig. 2(b)]. The polarization dependence of the absorption spectra of the BP$n$T ($n$=2,3) crystals are shown in Figs. 5(a) and 5(b). The bottom curves are $b$-polarized absorption spectra and the top curves are $a$-polarized ones. As predicted by the aggregate model, the lower Davydov exciton peaks in the BP$n$T ($n$=2,3) crystals are clearly polarized along the respective $b$ axis as shown in Figs. 5(a) and 5(b). Thus, by using the aggregate model, we can successfully interpret the intrinsic excitonic structures in the optical spectra of the BP$n$T ($n$=1–4) crystals.

## IV. SUMMARY

In summary, we have investigated the fundamental optical transitions of the intrinsic excitons in the co-oligomer crystals. Although only simple oligomer crystals such as OTs have so far been investigated, the co-oligomer crystals have been receiving considerable attention because of their good optical properties in recent years. In particular, the co-oligomer crystals exhibit not only good optical performance but also interesting fundamental properties. In fact, pronounced structures are observed in optical spectra of BP$n$T ($n$=1–4) crystals and they are assigned to the lower Davydov excitons. The excitons in BP1T and BP$n$T ($n$=2–4) crystals show optically forbidden and allowed features, respectively. The optical transition selection rules are different from those for OT crystals in spite of the similarity of the molecular symmetry. However, the selection rules for BP$n$T crystals can be well explained by using the aggregate model in the same manner as those for OT crystals. In the aggregate model, the optical transitions in BP$n$T crystals are interpreted to be driven by the constructive or destructive interference between the $\mu$'s of the two nonequivalent molecules

aligned like *H* aggregates. In the case of BP*n*T crystals, only $\mu_y$'s contribute to the optical transitions of the lower Davydov excitons by the interference, where the $\mu_y$'s are the projections of the $\mu$'s onto the *b* axes. The excitons in BP*n*T ($n=2,4$) and the BP1T crystal are optically allowed and forbidden because of the presence and the lack of the $\mu_y$'s, respectively, in the same manner as the even- and odd-numbered OTs. However, the exciton transition in the BP3T crystal is optically allowed and disagrees with those in odd-numbered OTs. Since the inclinations of the molecules in the direction of the *b* axis in the BP3T crystal are large compared to those of the other BP*n*Ts, the $\mu_y$'s remain despite it being an odd-numbered BP*n*T. These interpretations of the fundamental optical transitions in the co-oligomer crystals will be very useful for finding and developing oligomer materials having good optical properties.

## ACKNOWLEDGMENTS

This work has been partially supported by Grants-in-Aid for the Scientific Research in a Priority Area "Super-Hierarchical Structures" (Nos. 17067018 and 17067009), Nos. 18204028 and 19740175 from the Ministry of Education, Culture, Sports, Science and Technology of Japan, the Kurata Memorial Hitachi Science and Technology Foundation, and the Iketani Science and Technology Foundation.

*bando@sakura.cc.tsukuba.ac.jp

[1] D. Fichou, S. Delysse, and J.-M. Nunzi, Adv. Mater. (Weinheim, Ger.) **9**, 1178 (1997).
[2] G. Horowitz, P. Valat, F. Garnier, F. Kouki, and V. Wintgens, Opt. Mater. (Amsterdam, Neth.) **9**, 46 (1998).
[3] F. Meinardi, M. Cerminara, A. Sassella, R. Bonifacio, and R. Tubino, Phys. Rev. Lett. **91**, 247401 (2003).
[4] M. Muccini, E. Lunedei, A. Bree, G. Horowitz, F. Garnier, and C. Taliani, J. Chem. Phys. **108**, 7327 (1998).
[5] F. Kouki, P. Spearman, P. Valat, G. Horowitz, and F. Garnier, J. Chem. Phys. **113**, 385 (2000).
[6] M. A. Loi, C. Martin, H. R. Chandrasekhar, M. Chandrasekhar, W. Graupner, F. Garnier, A. Mura, and G. Bongiovanni, Phys. Rev. B **66**, 113102 (2002).
[7] M. Muccini, M. Schneider, C. Taliani, M. Sokolowski, E. Umbach, D. Beljonne, J. Cornil, and J. L. Brédas, Phys. Rev. B **62**, 6296 (2000).
[8] M. Muccini, E. Lunedei, C. Taliani, D. Beljionne, J. Cornil, and J. L. Brédas, J. Chem. Phys. **109**, 10513 (1998).
[9] F. C. Spano, Chem. Phys. Lett. **331**, 7 (2000).
[10] F. C. Spano, J. Chem. Phys. **114**, 5376 (2001).
[11] F. C. Spano, J. Chem. Phys. **116**, 5877 (2002).
[12] F. C. Spano, J. Chem. Phys. **118**, 981 (2003).
[13] F. Meinardi, M. Cerminara, A. Sassella, A. Borghesi, P. Spearman, G. Bongiovanni, A. Mura, and R. Tubino, Phys. Rev. Lett. **89**, 157403 (2002).
[14] F. Meinardi, S. Blumstengel, M. Cerminara, G. Macchi, and R. Tubino, Phys. Rev. B **72**, 035207 (2005).
[15] F. Meinardi, M. Cerminara, S. Blumstengel, A. Sassella, A. Borghesi, and R. Tubino, Phys. Rev. B **67**, 184205 (2003).
[16] H. Sun, Z. Zhao, F. C. Spano, D. Beljonne, J. Cornil, Z. Shuai, and J. L. Brédas, Adv. Mater. (Weinheim, Ger.) **15**, 818 (2003).
[17] S. Hotta, H. Kimura, S. A. Lee, and T. Tamaki, J. Heterocycl. Chem. **37**, 281 (2000).
[18] S. Hotta and T. Katagiri, J. Heterocycl. Chem. **40**, 845 (2003).
[19] S. Hotta and M. Goto, Adv. Mater. (Weinheim, Ger.) **14**, 498 (2002).
[20] S. Hotta, M. Goto, R. Azumi, M. Inoue, M. Ichikawa, and Y. Taniguchi, Chem. Mater. **16**, 237 (2004).
[21] M. Ichikawa, H. Yanagi, Y. Shimizu, S. Hotta, N. Suganuma, T. Koyama, and Y. Taniguchi, Adv. Mater. (Weinheim, Ger.) **14**, 1272 (2002).
[22] M. Ichikawa, R. Hibino, M. Inoue, T. Haritani, S. Hotta, T. Koyama, and Y. Taniguchi, Adv. Mater. (Weinheim, Ger.) **15**, 213 (2003).
[23] M. Nagawa, R. Hibino, S. Hotta, H. Yanagi, M. Ichikawa, T. Koyama, and Y. Taniguchi, Appl. Phys. Lett. **80**, 544 (2002).
[24] K. Bando, T. Nakamura, Y. Masumoto, F. Sasaki, S. Kobayashi, and S. Hotta, J. Appl. Phys. **99**, 013518 (2006).
[25] K. Shimizu, Y. Mori, and S. Hotta, J. Appl. Phys. **99**, 063505 (2006).
[26] M. Ichikawa, R. Hibino, M. Inoue, T. Haritani, S. Hotta, K. Araki, T. Koyama, and Y. Taniguchi, Adv. Mater. (Weinheim, Ger.) **17**, 2073 (2005).
[27] F. Sasaki, S. Kobayashi, S. Haraichi, H. Yanagi, S. Hotta, M. Ichikawa, and Y. Taniguchi, Jpn. J. Appl. Phys., Part 2 **45**, L1206 (2006).
[28] M. J. Frisch, G. W. Trucks, H. B. Schlegel, G. E. Scuseria, M. A. Robb, J. R. Cheeseman, J. A. Montgomery, Jr., T. Vreven, K. N. Kudin, J. C. Burant, J. M. Millam, S. S. Iyengar, J. Tomasi, V. Barone, B. Mennucci, M. Cossi, G. Scalmani, N. Rega, G. A. Petersson, H. Nakatsuji, M. Hada, M. Ehara, K. Toyota, R. Fukuda, J. Hasegawa, M. Ishida, T. Nakajima, Y. Honda, O. Kitao, H. Nakai, M. Klene, X. Li, J. E. Knox, H. P. Hratchian, J. B. Cross, C. Adamo, J. Jaramillo, R. Gomperts, R. E. Stratmann, O. Yazyev, A. J. Austin, R. Cammi, C. Pomelli, J. W. Ochterski, P. Y. Ayala, K. Morokuma, G. A. Voth, P. Salvador, J. J. Dannenberg, V. G. Zakrzewski, S. Dapprich, A. D. Daniels, M. C. Strain, O. Farkas, D. K. Malick, A. D. Rabuck, K. Raghavachari, J. B. Foresman, J. V. Ortiz, Q. Cui, A. G. Baboul, S. Clifford, J. Cioslowski, B. B. Stefanov, G. Liu, A. Liashenko, P. Piskorz, I. Komaromi, R. L. Martin, D. J. Fox, T. Keith, M. A. Al-Laham, C. Y. Peng, A. Nanayakkara, M. Challacombe, P. M. W. Gill, B. Johnson, W. Chen, M. W. Wong, C. Gonzalez, and J. A. Pople, GAUSSIAN 03, Revision C.02, Gaussian, Inc., Wallingford, CT, 2004.
[29] The Cambridge Structural Database, F. H. Allen, Acta Crystallogr., Sect. B: Struct. Sci. **58**, 380 (2002).
[30] H. Yanagi, A. Yoshiki, S. Hotta, and S. Kobayashi, J. Appl. Phys. **96**, 4240 (2004).
[31] M. Pope and C. E. Swenberg, *Electronic Processes in Organic Crystals* (Clarendon, Oxford, 1982).
[32] G. Horowitz, F. Kouki, A. El Kassmi, P. Valat, V. Wintgens, and F. Garnier, Adv. Mater. (Weinheim, Ger.) **11**, 234 (1999).
[33] F. C. Spano, Annu. Rev. Phys. Chem. **57**, 217 (2006).